

An Element Sensitive Saliency Model with Position Prior Learning for Web Pages

Jie Chang¹, Ya Zhang², Yanfeng Wang³
{j_chang, ya_zhang, yfwang}@sjtu.edu.cn

Cooperative Medianet Innovation Center (CMIC)
Shanghai Jiao Tong University

Abstract. Understanding human visual attention is important for multimedia applications. Many studies have attempted to learn from eye-tracking data and build computational saliency prediction models. However, limited efforts have been devoted to saliency prediction for Web pages, which are characterized by more diverse content elements and spatial layouts. In this paper, we propose a novel end-to-end deep generative saliency model for Web pages. To capture position biases introduced by page layouts, a Position Prior Learning sub-network is proposed, which models position biases as multivariate Gaussian distribution using variational auto-encoder. To model different elements of a Web page, a Multi Discriminative Region Detection (MDRD) branch and a Text Region Detection (TRD) branch are introduced, which target to extract discriminative localizations and “prominent” text regions likely to correspond to human attention, respectively. We validate the proposed model with FiWI, a public Web-page dataset, and shows that the proposed model outperforms the state-of-art models for Web-page saliency prediction.

Keywords: Web Viewing, Visual Attention, Variational Auto-Encoder

1 Introduction

Dominated by the “bottom-up” attentive mechanism of visual cognition [1], even without a specific goal, human vision system tends to focus on certain regions instead of randomly spreading. Modeling this human visual attention is essential for evaluating media designs. Inspired by the above visual attention mechanism, many computational *saliency models*, which attempt to predict salient regions of given media content, have been investigated. In building the saliency models, eye-tracking experiments have been leveraged as a dominant approach to collect training data.

Most existing saliency prediction studies focus on natural images [2,3]. Building upon the biological evidences [4,5], low-level features such as color, contrast, luminance, edge orientations or intensity are adopted to help predict human attention [6,7,8]. To capture the influence of content semantics, high-level features representing certain semantic concepts (e.g., faces, objects) are leveraged to further improve the prediction accuracy [9,10,11]. With the recent development of deep neural network, many efforts have been made to simultaneously

learn feature representations and saliency prediction models. Sparse coding is proposed to learn a multi-layer feature representation [12,13,14], and Convolutional Neural Networks (CNNs) attempt to learn both shallow and deep feature representations [15]. Furthermore, a feature weighting method is used to encode the combination of multi-layer feature maps extracted from CNN [16]. LSTM is leveraged to sequentially enhance the prediction accuracy of saliency model based on features extracted by deep neural networks [17]. More recently, adversarial training is leveraged to refine the predictive results of saliency model [18].

While much efforts have been devoted to saliency prediction of natural images, there have been very limited studies focusing on Web-page saliency [19,20,21]. Different from natural images, Web pages are rich in scattered salient stimuli (e.g., logos, text, graphs, picture) [22] of un-equivalent influence to human’s short-term attention [23]. It is thus more difficult to model human attention on Web pages, not only requiring more complicated feature representations but also modeling spatial layouts. Existing studies on Web-page saliency [19,20,21] mainly focus on exploring a better feature representation. However, they fail to take the characteristics of Web-page saliency into consideration. First, layout of Web pages greatly affect the deployment of human fixations, leading to a diverse set of reading patterns such as “F-shaped”, “layer-cake”, “spotted” and “commitment” [24,23,25]. The above studies for Web-page saliency tend to represent the *position-based visual preferences* using manually constructed position-bias maps, which is unable to adaptively reflect the accurate Web-page layout. Hence, we explore to model the position biases as a prior distribution which can be automatically learned from data. Second, different elements in Web pages usually have different influence on human attention. Different from natural images, there are many non-semantic elements in Web pages which may not grip human attention but unavoidably cause overmuch activated regions when we simple use a pre-trained CNN as a feature extractor, just as most previous works done. Instead, considering text and images are dominant elements in Web pages, we propose to adopt independent high-level semantic features for the two elements. We believe these feature representations are more consistent with human attention.

In our paper, we propose a deep generative saliency model for Web pages. The whole model consists of three sub-networks: Prior Learning Net (PL-Net) for modeling position biases, Element Feature Net (EF-Net) for extracting representations for different elements, and Prediction Net(P-Net) for generating the final saliency map. The PL-Net leverages a VAE-based Position Prior Learning (PPL) algorithm to automatically learn position biases of user viewing behaviors and no longer depends on pre-defined position bias maps as previous methods. PPL employs variational auto-encoder to model position biases as multivariate Gaussian distribution. The EF-Net contains three branches. In addition to an overall feature branch, a Multi Discriminative Region Detection (MDRD) branch and a Text Region Detection(TRD) branch are introduced. MDRD is proposed to extract discriminative localizations which are likely to correspond to human attention, thus reducing the spatially irrelevant activation produced by trivial

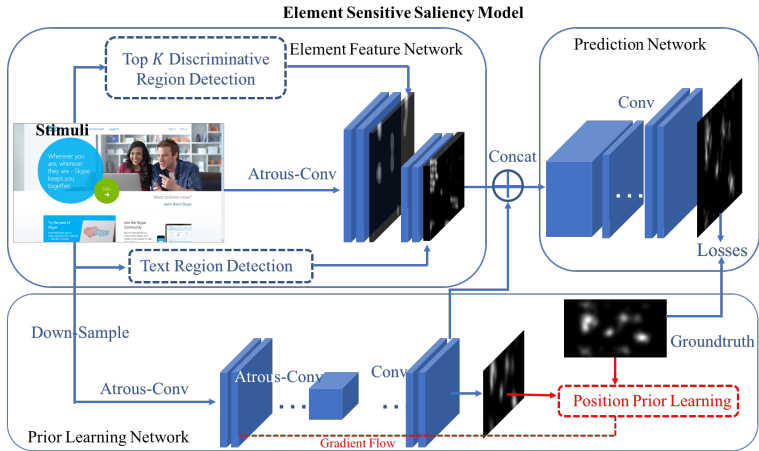


Fig. 1. An overview of Element Sensitive Saliency Model with Position Prior Learning.

elements. This branch can be seen as a pre-filter to reduce the “noise” distraction from low-level features. TRD branch is essentially a text/background classifier to extract text saliency map from Web pages. The extracted text saliency map represents the regions corresponding “prominent” text (e.g., logos, headlines/subheading, WordArt). The whole model we proposed is a deep generative model which can be trained end-to-end. By experimenting on FiWi, a released Web-page dataset, our proposed algorithms distinguish our model and boost the performance of saliency prediction.

The main contributions of our studies are summarized as follows.

- We model the diverse *visual preference* caused by page layouts with a VAE-based Position Prior Learning.
- We explore element-based feature representations and leverage a MDRD branch and a TRD branch to capture the impact of images and text to human attention.
- Experimental studies have shown that the proposed method outperforms the state-of-art models for Web-page saliency prediction.
- We also experimentally verifies the proposed TRD and MDRD can be plugged into other models to boost their performance.

2 Method

Figure 1 provides an overview of the proposed generative saliency model for Web pages, which consists of three sub-networks: Prior Learning Net (PL-Net) for modeling position biases, Element Feature Net (EF-Net) for extracting features for different elements, and Prediction Net (P-Net) for generating the final

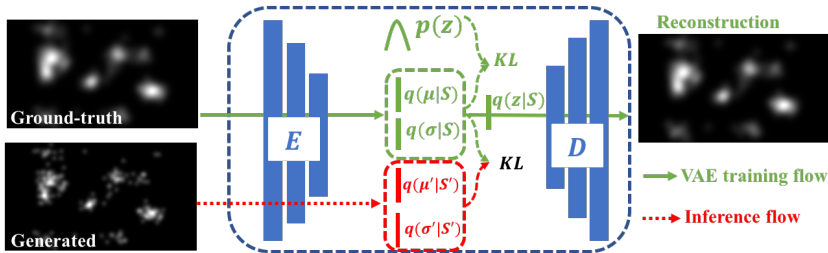


Fig. 2. The architecture of Position Prior Learning (PPL) sub-network. The corresponding ground-truth of the trained stimulus is reconstructed by a variational auto-encoder for a learned posterior distribution. Meanwhile another latent distribution inferred from the generated prior map of PL-Net is aligned with the previous learned posterior by KL divergence term (marked in black).

saliency map. In PL-Net, a VAE-based Position Prior Learning (PPL) algorithm is leveraged to model position biases as multivariate Gaussian distribution. In EF-Net, we integrate extra Multi Discriminative Region Detection (MDRD) branch and Text Region Detection (TRD) branch to extract better representations which are more consistent with human attention. The representations from PL-Net and EF-Net are fused in P-Net to generate the final saliency map. In the rest of this section, we present PPL, MDRD and TRD in details.

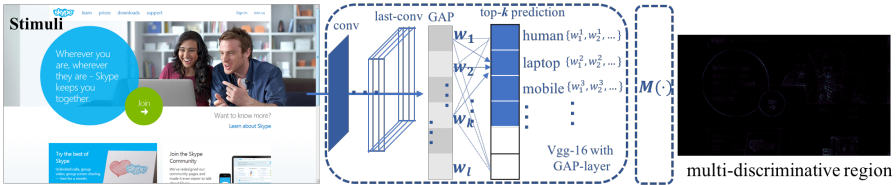
2.1 Position Prior Learning

To predict Web page saliency, it is important to model position biases introduced by page layouts. Unlike previous studies which adopt fixed position bias maps manually constructed beforehand, we propose a Position Prior Learning (PPL) algorithm based on Variational Auto-Encoder (VAE) [26] to automatically learn such position biases. Based on the observation that similar position biases occurred on corresponding Web pages sharing similar layouts. We explore to model these position biases as the mean and standard deviation of multivariate Gaussian distribution which are learned as latent variables in VAE (see Fig 2). Specifically, a set of true saliency maps S are used to optimize a VAE network including an encoder E and a decoder D for obtaining the posterior distribution $q(z|S)$. This training procedure follows the objective function below:

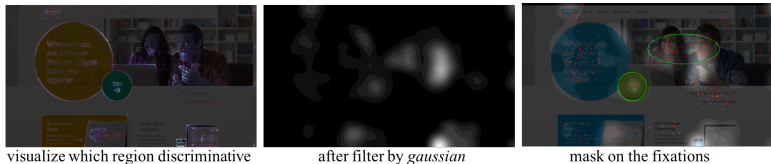
$$L(\theta, \phi; S) = \lambda_1 \mathbb{E}_{z \sim q_\phi(z|S)} [\log p_\theta(S|z)] - \lambda_2 D_{KL}(q_\phi(z|S) || p(z)), \quad (1)$$

where θ and ϕ are respective parameters in encoder E and decoder D of VAE, $p(z)$ is a standard normal prior, $N(\mathbf{0}, \mathbf{I})$, λ_1 and λ_2 control the weights of the expectation term and KL-divergence terms. The learned variational approximate posterior can be formulated as a multivariate Gaussian with a diagonal covariance structure,

$$q_\phi(z|S) = N(z; \mu, \sigma^2 \mathbf{I} | S), \quad (2)$$



(a) Multi-Discriminative Region Detection (MDRD)



(b)

Fig. 3. (a) Multi-Discriminative Region Detection: a pretrained Vgg16-CAM model with GAP-layer [27] is used to predict the top- K class in the stimulus. (b) Visualization of relevant results of MDRD. Left: the initial discriminative representation; Middle: discriminative region mapping after Gaussian blurring; Right: regions in green circle illustrate the highly correlation between extracted regions and human fixations (red dots).

where the mean and standard deviation of the approximate posterior, $\boldsymbol{\mu}^{(i)}$ and $\boldsymbol{\sigma}^{(i)}$, are outputs of the encoding MLP (E).

Meanwhile, the generated prior maps S' from PL-Net are fed into the parameter-sharing encoder E . We also let the output of E be a multivariate Gaussian structure,

$$q_{\phi}(\mathbf{z}' | S') = N(\mathbf{z}' ; \boldsymbol{\mu}', \boldsymbol{\sigma}'^2 \mathbf{I} | S'), \quad (3)$$

where ϕ are reused parameters of encoder E .

Then another KL-divergence representing the discrepancy between the above two approximate posterior, $q_{\phi}(\mathbf{z} | S)$ and $q_{\phi}(\mathbf{z}' | S')$,

$$L(\theta_{pl}) = D_{KL}(N(\mathbf{z}' ; \boldsymbol{\mu}', \boldsymbol{\sigma}'^2 \mathbf{I} | S') || N(\mathbf{z}; \boldsymbol{\mu}, \boldsymbol{\sigma}^2 \mathbf{I} | S)) \quad (4)$$

is calculated as the loss for training PL-Net so as to enable prior maps generated by PL-Net to possess similar latent variables with that of true saliency maps. θ_{pl} indicates the parameters in PL-Net.

2.2 Multi Discriminative Region Detection

Many previous works directly leverage feature maps extracted by pre-trained CNNs as the high-level representations for saliency prediction. While this approach performs not well for the specified Web pages which usually contain

various design elements since it makes the extracted feature maps contain over-much activation regions. However, human fixations can not be guided to each element of a Web page within just a few seconds, which means the previous extracted feature maps contain lots of redundant information.

Inspired by class activation mapping proposed in [27], we propose Multiple Discriminative Region Detection (MDRD) to extract the remarkable object regions where human maybe easily focus on (see Fig 3). Specifically, different from the direct feature extraction used before, an auxiliary classification is performed on webpage by reusing the VGG16-CAM model trained on ImageNet [28]. We then select top- K categories predicted from one Web page.

$$Y_c = \frac{\exp \sum_{x,y} \sum_l w_l^c f_l(x,y)}{\sum_c \exp(\sum_{x,y} \sum_l w_l^c f_l(x,y))}; \quad k \in \{\mathbf{c} \mathbf{Top}_K(Y_c, c = 1, 2, \dots, \#)\} \quad (5)$$

where Y_c is the probabilistic value w.r.t class c ; $f_l(x,y)$ represents the activation of unit l in the last convolutional layer at spatial location (x,y) ; w_l^c is the weights connected after the global average pooling (GAP) layer w.r.t c ; $\#$ is the number of all categories in ImageNet; \mathbf{Top}_K is defined as the function which return a set of class numbers whose predicted scores are in top- K . K is determined by the number of dominated eigenvalues after PCA implemented on the last convolutional layers.

Then For each category k within top- K , we fetch a set of weights w.r.t k class, w_l^k , map them back to the last convolutional layers to generated a single class discriminative region mapping $S_k(x,y)$:

$$S_k(x,y) = \sum_l w_l^k f_l(x,y), \quad (6)$$

$M(\cdot)$ is the fusion function to mixed the K discriminative region mappings for obtaining a multi-discriminative region mapping $M(x,y)$:

$$M(x,y) = \frac{1}{N} \sum_{k=1}^K S_k(x,y) = \frac{1}{N} \sum_{k=1}^K \sum_l w_l^k f_l(x,y). \quad (7)$$

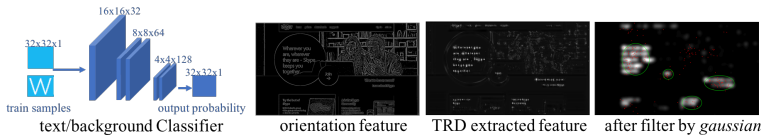
We can find highly positive correlations between the feature maps extracted by MDRD and where human fixations located (see Fig 3-b).

2.3 Text Region Detection

Web pages are rich in text information which greatly attracted human fixations but few of existing models considered text information specifically. Our proposed Text Region Detection (TRD), however, aims to generate representation for prominent text information. TRD is mainly implemented by a Text/Background Classifier (C_f) which can be independently trained on the typical dataset (ICDAR, SVT) released for character recognition (we introduce these datasets in section 3.1). The structure of C_f is simply consisted with 4 conv-layers and the



(a) Text Region Detection (TRD)



(b)

Fig. 4. (a) shows us the procedure of Text Region Detection: a Text/Background Classifier (C_f) slides around on the stimuli with different scale, the result of each window-sliding is scaled to the same resolution for the average fusion and Gaussian blurring. (b), column-1: illustration of C_f structure; column-2: text representation generated by orientation feature [21]; column-3: text representation generated by our TRD; column-4: final text saliency map after Gaussian blurring. We mask human fixations (red dots) of this webpage on the text saliency map, which visualizes the strong correlation (circled in green).

last conv-layer is connected to output the text/background probability of the input patch (see Fig 4-b). C_f can be trained independently by optimizing the loss function below:

$$\theta_{C_f} = \arg \max \mathbb{E}_{(x,c)} [-c \cdot (\log(p(c|x))) - (1-c) \cdot \log(1-p(c|x))], \quad (8)$$

where x are text and non-text patches cropped from above annotated character datasets; $c \in \{text, background\}$ can be formulated by $\{1, 0\}$; $p(c|x)$ is the probabilistic output of the binary classifier and θ_{C_f} are parameters in classifier C_f .

A well-trained C_f is then performed around the input stimulus by sliding window for generating a text response map which is appropriately padded to a same resolution. Particularly, since C_f is pre-trained on dataset with fixed resolution, we repeat this process for 4 different scales by resizing the raw stimulus with the factor of 0.2, 0.5, 1.5 and 2 so that text with different size can be detected as possible (see Fig 4-a). The output T of TRD is further converted into a probability distribution over the feature map by the means of a softmax and then filtered by Gaussian to regularize the final text saliency map:

$$p(m,n) = \frac{\exp(T(m,n))}{\sum_{m,n} \exp(T(m,n))} * G_\sigma, \quad (9)$$

where σ in the Gaussian filter G is properly set to 10 (larger σ makes more highlighted region while too small σ makes disconnected highlighted regions); (m, n) indicates the pixel coordinates in T .

For comparison, we also illustrate the text representation extracted from traditional low-level feature in Fig 4-b, from which we can see TRD can depress non-text elements in Web page and obtain more appropriate textual regions more consistent with the deployment of human fixations.

2.4 Loss Function

The feature maps from PL-Net and EF-Net are concatenated together as the input of Prediction Network (P-Net). P-Net generates the final predicted saliency map based on stacked CNN structure. The loss function we defined between the predicted saliency map and its corresponding ground-truth is the linear combination of two terms as follows:

$$L(\theta^*) = \alpha L_1(\hat{S}, S) + \beta L_2(\hat{S}, S), \quad (10)$$

where θ^* are training parameters in EF-Net and P-Net; \hat{S} are predicted saliency maps from P-Net and S are corresponding ground-truth; α, β are hyper-parameters to trade-off two loss terms where L_1 is defined as the cross entropy loss:

$$L_1(\hat{S}, S) = \mathbb{E}_{s, \hat{s}}[S \log(\hat{S}) - (1 - S) \log(1 - \hat{S})], \quad (11)$$

and L_2 is defined as the KL-divergence measuring the loss of information when distribution \hat{S} is used to approximate the distribution S :

$$L_2(\hat{S}, S) = \sum_i \hat{S}_i \log\left(\frac{\hat{S}_i}{S_i + \varepsilon} + \varepsilon\right), \quad (12)$$

where i indicates the i^{th} pixel in both saliency maps and ε is a regularization constant.

3 Experiments Setup

3.1 Datasets & Evaluation Introduction

FiWI is a dataset proposed in [19], which contains 149 Web page screenshots with eye-tracking fixation data collected from 11 observers. The observation is short-term as well as free-viewing to ensure the visual preference being driven by “bottom-up” visual mechanism. FiWI is categorized as Pictorial(50), Textual(50) and Mixed(49) images according to the different composition of text and pictures. Pictorial Web pages are occupied by pictures and less text, Textual Web pages contains informative text with high density and Mixed Web pages are a mix of pictures and text.

Character Datasets are used for training the text/background classifier C_f for TRD proposed in section 2.3. They are released datasets including IC-DAR 2003 [29] containing photos with scene text of the world and the Street View Text (SVT) [30] containing images downloaded from Google Street View of road-side scenes automatically annotated cropped characters. And we manually generate non-text samples from ICDAR 2003 as the negative training data for text/background classifier C_f .

Evaluation Metrics For evaluating our performance quantitatively, three similarity metrics¹ are adopted including Linear Correlation Coefficient (CC), Normalized Scanpath Saliency (NSS) and shuffled Area Under Curve (sAUC) [31]. We also use AUC for plotting the comparison results intuitively.

3.2 Implementation Detail

Element Feature Network (EF-Net) operates on the original stimulus with 1360×768 resolution, followed by a sequence of atrous conv-layer groups and max pooling layers. Atrous convolution (also named as dilated convolution [32]), which has been successfully applied to semantic segmentation [33,34], could increase the receptive field of images while preserving the scale at the same time. Additionally, atrous convolution leads to less kernel parameters when enables larger receptive field. In atrous-conv, the filter is 3×3 with stride 1 and the dilated rate is 3. 2×2 Max pooling is used between two atrous-conv groups. Feature maps are down-sampled to $W-340 \times H-192 \times C-256$ in EF-Net before the concatenation with the feature maps generated from PL-Net. PL-Net operates on the $4 \times$ down-sampling stimulus with 340×192 followed by 3 atrous-conv layers until to 42×24 scale. The up-sampling part of PL-Net is consisted with a sequence of conv-layers and deconv-layer to a generated prior maps S' with 340×192 resolution. The penultimate feature mas ($W-340 \times H-192 \times C-128$) of PL-Net is concatenated with feature maps in EF-Net (see Fig 1). The dimension of latent code in the proposed VAE-based Position Prior Learning is set to 100. λ_1 and λ_2 in Eq 8 are both set to 1. And the hyper-parameters of loss function in Eq 10 are set to $\alpha = 1$, $\beta = 0.1$ and $\epsilon = 10^{-6}$ in Eq 12.

4 Experiments Results

In this section, we first qualitatively evaluate our model with existing nine studies proposed for saliency prediction. We also present a quantitative comparison on Pictorial, Text and Mixed images from FiWI. Furthermore, we analyze the effectiveness of each component of the proposed algorithm by removing position prior learning (PPL), multi-discriminative region detection (MDRD) and text region detection (TRD) from the whole network. Last, we experimentally verifies that the proposed TRD and MDRD can be plugged into other saliency models and we show that they lead to performance gains on top of two state-of-art saliency models, Sam [17] and Mlnet [16].

¹ <https://sites.google.com/site/saliencyevaluation/evaluation-measures>

4.1 Performance Comparison

We compare our model with nine previous saliency models, including: MMF [21], MKL [19], AIM [35], SIG [36], SUN [31], GBVS [8], Itti [7], Sam [17] and Mlnet [16]. Figure 5 illustrates the comparison results among the models, which demonstrates that our model better represents human attention. In Table 1, we quantitatively compare the performance in terms of three evaluation metrics (sAUC, NSS and CC) for Pictorial/Text/Mixed Web pages. It can be seen that our model greatly outperforms other baselines in Pictorial&Text Web pages and is slightly better in Mixed Web pages.

Table 1. Quantitative Measurements

Model	Pictorial-webpage			Text-webpage			Mixed-webpage		
	sAUC	NSS	CC	sAUC	NSS	CC	sAUC	NSS	CC
Itti [7]	0.538	0.443	0.233	0.544	0.483	0.234	0.552	0.462	0.267
GBVS [8]	0.564	0.685	0.350	0.561	0.680	0.329	0.575	0.708	0.336
AWS [37]	0.633	0.806	0.401	0.648	0.867	0.406	0.645	0.854	0.393
Signat [36]	0.664	0.848	0.415	0.682	0.885	0.408	0.682	0.920	0.410
AIM [35]	0.663	0.907	0.453	0.679	0.936	0.445	0.678	0.943	0.439
SUN [31]	0.707	1.072	0.488	0.687	0.993	0.459	0.700	1.017	0.490
MKL [19]	0.723	0.880	0.429	0.741	0.861	0.410	0.730	0.891	0.433
MMF [21]	0.731	0.904	0.441	0.720	0.890	0.419	0.760	0.920	0.431
Mlnet [16]	0.703	0.912	0.530	0.711	0.802	0.463	0.725	0.905	0.522
Sam [17]	0.720	0.982	0.494	0.743	0.924	0.470	0.762	0.938	0.500
Ours	0.761	1.202	0.641	0.781	1.250	0.511	0.751	1.029	0.580

4.2 Analysis of Each Module

We further analyze the respective effect of PPL, MDRD and TRD proposed in our Element Sensitive Saliency Model. First, to explore whether Position Prior Learning captures position bias in web page viewing, we illustrate in Fig 6 with three kinds of Web pages: web pages rich in text information, web pages arranged by pictures, and web pages combined with pictures and text. For each category, we average their corresponding prior maps S' generated by Prior Learning Network and we observe typical “F-shaped” and “top-left” bias in textual web pages; “center-around” bias in pictorial images; “sidebar” and “top-left” bias in mixed web pages. That means the proposed PPL algorithm is able to capture common prior of position bias for Web pages with similar layouts.

Then we intuitively visualize what TRD and MDRD extracted from original Web pages in figure 7. Representation from TRD shows that TRD selectively highlights locations where textual information is remarkable instead of simply detecting the edge lines of each character used in previous method. We see text

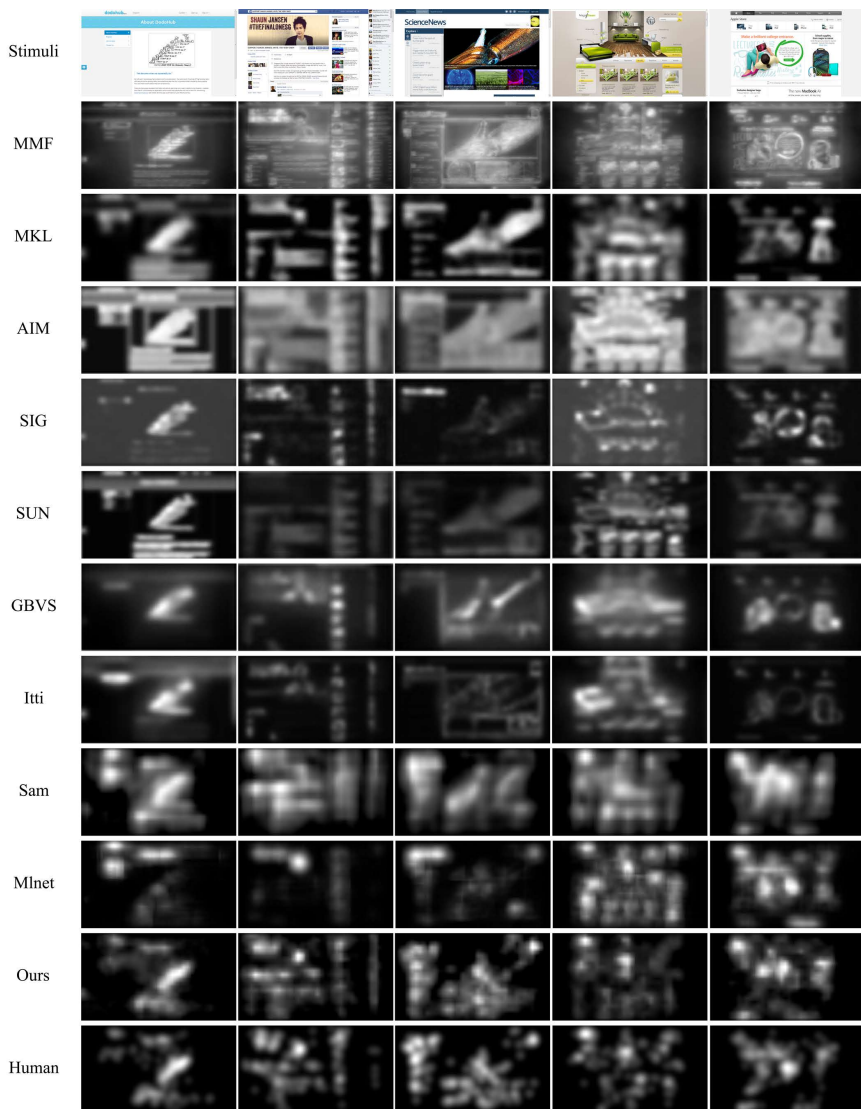


Fig. 5. Qualitative results and comparison to the state of the art. Compared with MMF and MKL without considering “prominent” text information, our predicted saliency maps have more accurate response at textual location. We also outperform other baselines (AIM~Mlnet) proposed for natural images by avoiding patches of irrelevant high-response.

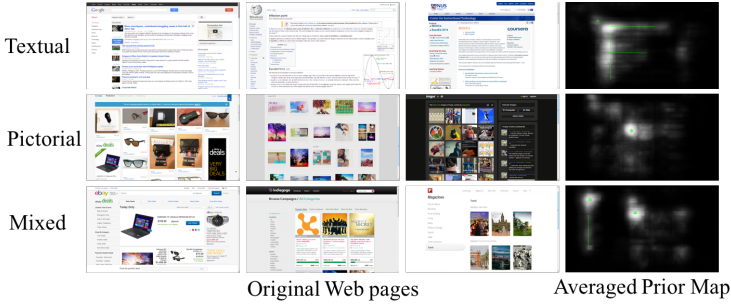


Fig. 6. Visualization of the typical position biases learned by Prior Learning Network. Last column shows the corresponding averaged results generated from Prior Learning Network for each kind of Web pages.

in logos, headlines or subheadings have larger activation on text saliency maps, which is important for our model since human usually pay more attention on these regions than normal text in main bodies. Representation from MDRD also shows that the proposed MDRD could “pre-select” some special discriminative regions while suppress textual regions greatly. For comparison, as most previous works done, representation from pooling5 is extracted from pre-trained VGG16 [38], which shows feature maps generated by our MDRD are more sparse with most inconspicuous regions suppressed.

Furthermore, we experimentally illustrate the influence of TRD/MDRD/PPL in Figure 8. We overlay the predicted saliency maps on the original Web pages for a better intuitive comparison and we find “Base” model usually causes over-much highlighted regions while the others could make specific locations stand out. PPL could shrink the scope of predicted salient regions to approximate true distribution as well as some position bias. AUC evaluation is also used for quantitatively measures effect of respective module. Table 2 quantitatively compares “Base”, “Base+TRD”, “Base+MDRD”, “Base+TRD+MDRD” and the proposed model, “Base+TRD+MDRD+PPL”, in terms of sAUC, NSS and CC metrics, which shows each module greatly contributes to saliency prediction for Web pages.

Last, we experimentally verifies that our proposed TRD and MDRD can be used to boost the performance of two state-of-art works Sam [17] and Mlnet [16]. Fig 9 shows that with introduction of TRD and MDRD, all metrics increase, especially for NSS and CC.

5 Conclusion

In this paper, we present a Element Sensitive Saliency Model for Web pages. The whole model consists of Element Feature Network (EF-Net), Prior Learning Network (PL-Net) and Prediction Network (P-Net). Compared with previous works, we propose VAE-based Position Prior Learning in PL-Net to automatically learn

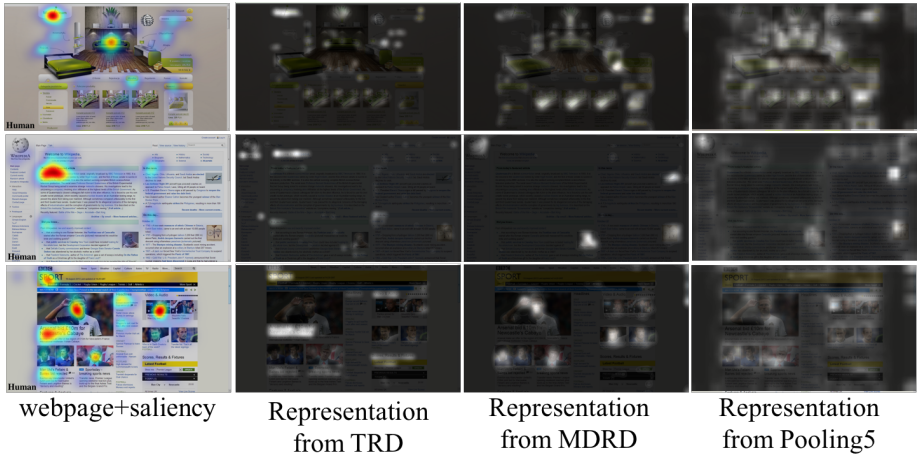


Fig. 7. Visualization of what TRD and MDRD extracted. Column-1(left): Stimuli with overlaying heatmap of human attention; column-2: representations extracted from TRD; column-3: representations extracted from MDRD; column-4(right): representations directly extracted from pooling5 in pre-trained VGG16.

Table 2. Quantitative Measurements

Prunning Experiment	All Test Webpages		
	sAUC	NSS	CC
Baseline	0.545	0.561	0.402
Baseline+TRD	0.730	0.855	0.511
Baseline+MDRD	0.700	0.820	0.495
Baseline+TRD+MDRD	0.731	1.005	0.612
Baseline+TRD+MDRD+PPL	0.760	1.085	0.637

the various visual preference when human scan Web pages. Additionally, in EF-Net, we leverage Text Region Detection(TRD) and Multi-Discriminative Region Detection(MDRD) to handle specific challenges in this task. We experimentally verified that the proposed model outperforms the state-of-art models for Web-page saliency prediction.

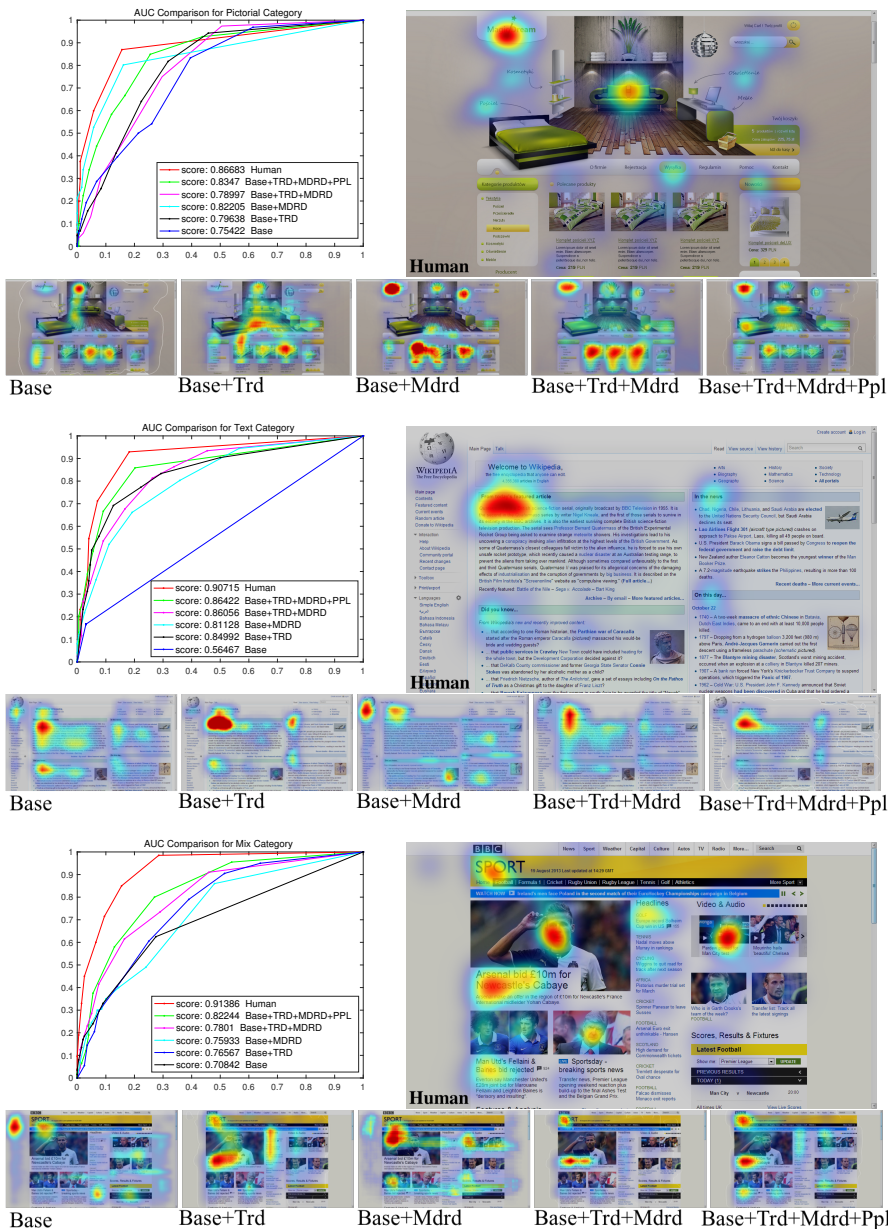


Fig. 8. Qualitative results under different configuration. “Base” denotes most simple architecture without TRD, MDRD and PPL. “Base+Trd” means we just introduce TRD branch, “Base+Mdrd” means we just introduce MDRD branch, “Base+Trd+Mdrd” means we just remove Position Prior Learning and “Base+Trd+Mdrd+Ppl” means the whole model.

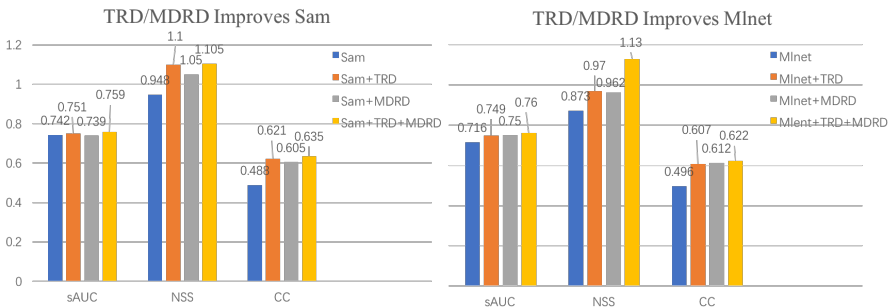


Fig. 9. Quantitative comparison when we introduce TRD and MDRD in Sam [17] and Mlnet [16].

References

1. Rensink, R.A.: The dynamic representation of scenes. *Visual cognition* **7**(1-3) (2000) 17–42
2. Bylinskii, Z., Judd, T., Borji, A., Itti, L., Durand, F., Oliva, A., Torralba, A.: Mit saliency benchmark
3. Borji, A., Itti, L.: Cat2000: A large scale fixation dataset for boosting saliency research. *CVPR 2015 workshop on "Future of Datasets"* (2015) arXiv preprint arXiv:1505.03581.
4. Zhaoping, L.: Attention capture by eye of origin singletons even without awareness a hallmark of a bottom-up saliency map in the primary visual cortex. *Journal of Vision* **8**(5) (2008) 1–1
5. Zhang, X., Zhaoping, L., Zhou, T., Fang, F.: Neural activities in v1 create a bottom-up saliency map. *Neuron* **73**(1) (2012) 183–192
6. Itti, L., Koch, C., Niebur, E.: A model of saliency-based visual attention for rapid scene analysis. *IEEE Transactions on pattern analysis and machine intelligence* **20**(11) (1998) 1254–1259
7. Itti, L., Koch, C.: A saliency-based search mechanism for overt and covert shifts of visual attention. *Vision Research* **40**(12) (2000) 1489–1506
8. Harel, J., Koch, C., Perona, P.: Graph-based visual saliency. In: *Advances in neural information processing systems*. (2007) 545–552
9. Cerf, M., Harel, J., Einhäuser, W., Koch, C.: Predicting human gaze using low-level saliency combined with face detection. In: *Advances in neural information processing systems*. (2008) 241–248
10. Einhäuser, W., Spain, M., Perona, P.: Objects predict fixations better than early saliency. *Journal of Vision* **8**(14) (2008) 18–18
11. Judd, T., Ehinger, K., Durand, F., Torralba, A.: Learning to predict where humans look. In: *Computer Vision, 2009 IEEE 12th international conference on, IEEE* (2009) 2106–2113
12. Borji, A., Itti, L.: Exploiting local and global patch rarities for saliency detection. In: *Computer Vision and Pattern Recognition*. (2012) 478–485
13. Shen, C., Zhao, Q.: Learning to predict eye fixations for semantic contents using multi-layer sparse network. *Neurocomputing* **138** (2014) 61–68
14. Shen, C., Song, M., Zhao, Q.: Learning high-level concepts by training a deep network on eye fixations. In: *NIPS Deep Learning and Unsup Feat Learn Workshop. Volume 2*. (2012)
15. Pan, J., Sayrol, E., Giroinieto, X., Mcguinness, K., Oconnor, N.E.: Shallow and deep convolutional networks for saliency prediction. In: *Computer Vision and Pattern Recognition*. (2016) 598–606
16. Cornia, M., Baraldi, L., Serra, G., Cucchiara, R.: A deep multi-level network for saliency prediction. In: *Pattern Recognition (ICPR), 2016 23rd International Conference on, IEEE* (2016) 3488–3493
17. Cornia, M., Baraldi, L., Serra, G., Cucchiara, R.: Predicting human eye fixations via an lstm-based saliency attentive model. arXiv preprint arXiv:1611.09571 (2016)
18. Pan, J., Canton, C., McGuinness, K., O'Connor, N.E., Torres, J., Sayrol, E., Giroi Nieto, X.: Salgan: Visual saliency prediction with generative adversarial networks. arXiv preprint arXiv:1701.01081 (2017)
19. Shen, C., Zhao, Q.: Webpage saliency. In: *European conference on computer vision, Springer* (2014) 33–46

20. Shen, C., Huang, X., Zhao, Q.: Predicting eye fixations on webpage with an ensemble of early features and high-level representations from deep network. *IEEE Transactions on Multimedia* **17**(11) (2015) 2084–2093
21. Li, J., Su, L., Wu, B., Pang, J., Wang, C., Wu, Z., Huang, Q.: Webpage saliency prediction with multi-features fusion. In: *Image Processing (ICIP), 2016 IEEE International Conference on*, IEEE (2016) 674–678
22. Still, J.D., Masciocchi, C.M.: A saliency model predicts fixations in web interfaces. In: *5 th International Workshop on Model Driven Development of Advanced User Interfaces (MDDAUI 2010)*, Citeseer (2010) 25
23. Buscher, G., Cutrell, E., Morris, M.R.: What do you see when you're surfing?: using eye tracking to predict salient regions of web pages. In: *Proceedings of the SIGCHI conference on human factors in computing systems*, ACM (2009) 21–30
24. Pernice, K., Whittenton, K., Nielsen, J.: *How People Read on the Web: The Eye-tracking Evidence*. Nielsen Norman Group (2014)
25. Jakob, N.: *F-shaped pattern for reading web content*. Alertbox: Current Issues in Web Usability (2006)
26. Kingma, D.P., Welling, M.: Auto-encoding variational bayes. *arXiv preprint arXiv:1312.6114* (2013)
27. Zhou, B., Khosla, A., Lapedriza, A., Oliva, A., Torralba, A.: Learning deep features for discriminative localization. In: *Computer Vision and Pattern Recognition (CVPR), 2016 IEEE Conference on*, IEEE (2016) 2921–2929
28. Krizhevsky, A., Sutskever, I., Hinton, G.E.: Imagenet classification with deep convolutional neural networks. In: *Advances in neural information processing systems*. (2012) 1097–1105
29. <http://algoval.essex.ac.uk/icdar/datasets.html>
30. Wang, K., Belongie, S.: Word spotting in the wild. In: *European Conference on Computer Vision*, Springer (2010) 591–604
31. Zhang, L., Tong, M.H., Marks, T.K., Shan, H., Cottrell, G.W.: Sun: A bayesian framework for saliency using natural statistics. *Journal of vision* **8**(7) (2008) 32–32
32. Yu, F., Koltun, V.: Multi-scale context aggregation by dilated convolutions. *arXiv preprint arXiv:1511.07122* (2015)
33. Wang, P., Chen, P., Yuan, Y., Liu, D., Huang, Z., Hou, X., Cottrell, G.: Understanding convolution for semantic segmentation. *arXiv preprint arXiv:1702.08502* (2017)
34. Chen, L.C., Papandreou, G., Kokkinos, I., Murphy, K., Yuille, A.L.: Deeplab: Semantic image segmentation with deep convolutional nets, atrous convolution, and fully connected crfs. *arXiv preprint arXiv:1606.00915* (2016)
35. Bruce, N.D., Tsotsos, J.K.: Saliency, attention, and visual search: An information theoretic approach. *Journal of vision* **9**(3) (2009) 5–5
36. Hou, X., Harel, J., Koch, C.: Image signature: Highlighting sparse salient regions. *IEEE transactions on pattern analysis and machine intelligence* **34**(1) (2012) 194–201
37. Garcia-Diaz, A., Leboran, V., Fdez-Vidal, X.R., Pardo, X.M.: On the relationship between optical variability, visual saliency, and eye fixations: A computational approach. *Journal of vision* **12**(6) (2012) 17–17
38. Simonyan, K., Zisserman, A.: Very deep convolutional networks for large-scale image recognition. *arXiv preprint arXiv:1409.1556* (2014)